The Journal of Experimental Biology 208, 157-168
Published by The Company of Biologists 2005
doi:10.1242/jeb.01332

Tympanal travelling waves in migratory locusts

James F. C. Windmill[1,*], Martin C. Göpfert[2] and Daniel Robert[1]

[1]*School of Biological Sciences, University of Bristol, Woodland Road, Bristol, BS8 1UG, UK* and [2]*Volkswagen-Foundation-research group, Institute of Zoology, University of Cologne, Weyertal, 119 50923, Cologne, Germany*

*Author for correspondence (e-mail: james.windmill@bristol.ac.uk)

Accepted 5 October 2004

Summary

Hearing animals, including many vertebrates and insects, have the capacity to analyse the frequency composition of sound. In mammals, frequency analysis relies on the mechanical response of the basilar membrane in the cochlear duct. These vibrations take the form of a slow vibrational wave propagating along the basilar membrane from base to apex. Known as von Békésy's travelling wave, this wave displays amplitude maxima at frequency-specific locations along the basilar membrane, providing a spatial map of the frequency of sound – a tonotopy. In their structure, insect auditory systems may not be as sophisticated as those of mammals, yet some are known to perform sound frequency analysis. In the desert locust, this analysis arises from the mechanical properties of the tympanal membrane. In effect, the spatial decomposition of incident sound into discrete frequency components involves a tympanal travelling wave that funnels mechanical energy to specific tympanal locations, where distinct groups of mechanoreceptor neurones project. Notably, observed tympanal deflections differ from those predicted by drum theory. Although phenomenologically equivalent, von Békésy's and the locust's waves differ in their physical implementation. von Békésy's wave is born from interactions between the anisotropic basilar membrane and the surrounding incompressible fluids, whereas the locust's wave rides on an anisotropic membrane suspended in air. The locust's ear thus combines in one structure the functions of sound reception and frequency decomposition.

Supplementary material available online at
http://jeb.biologists.org/cgi/content/full/208/1/157/DC1

Key words: bioacoustics, frequency detection, hearing, travelling wave, tympanum, locust.

Introduction

A salient feature of many auditory systems is their capacity to encode the frequency composition of acoustic waves. In a series of ingenious experiments, Georg von Békésy established the physical basis of frequency discrimination in the mammalian ear. He demonstrated that the capacity of the ear to decipher the tonal composition of sounds relies on the particular physical properties of the basilar membrane in the cochlea (von Békésy 1960). This work established that frequency analysis is based on the spatial mapping of sound frequencies along the basilar membrane. This mapping is brought about by sound-induced mechanical displacements of the basilar membrane that take the shape of travelling waves. These waves are much slower, by several orders of magnitude, than ordinary pressure waves that pass through the cochlea (Nobili et al., 1998). The progression of the travelling waves along the cochlea is also notable by the fact that the wave speed is not constant (Serbetcioglu and Parker, 1999; Rhode and Recio, 2000; Ren, 2002). In effect, as the wave propagates along the cochlea, from the base to the apex, the speed of its propagation gradually diminishes while its amplitude of vibration increases (Fig. 1). At a certain location the wave's amplitude reaches a maximum, and then rapidly attenuates (Fig. 1A). At that location, the mechanical response also exhibits a phase lag that is much greater than that of a simple resonator (Fig. 1B). Crucially, the exact location at which these events take place is frequency specific, a characteristic that is due to the interaction of the incompressible fluids in the cochlear duct and the anisotropic nature of the basilar membrane (Olson and Mountain, 1991; Olson, 1999; for a recent review see Robles and Ruggero, 2001). This is the physical basis for the topographic representation of sound; also referred to as tonotopy, or the place principle.

The ears of locusts and grasshoppers (Orthoptera: acrididae) have been known and studied for quite some time (Schwabe, 1906; Autrum, 1941; Gray, 1960; Michelsen, 1971) and their structure and function are among the better known in insects. The main anatomical components of locust ears are an external tympanal membrane (TM) and a mechanosensory organ – Müller's organ – that contains four clusters of multicellular mechanoreceptive units: the scolopidia (Gray, 1960). It was also established, using electrophysiological techniques, that the ears of locusts could perform some form of frequency

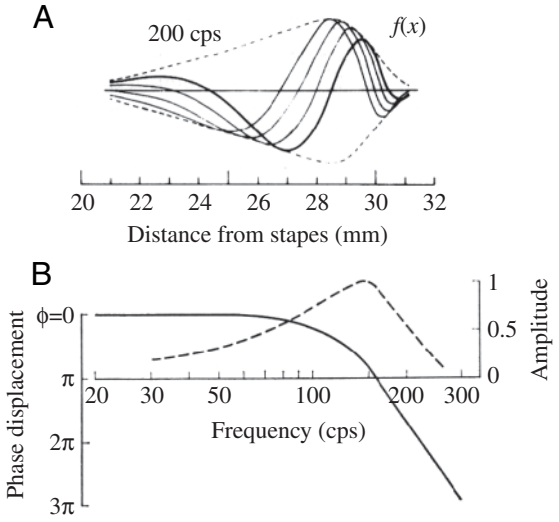

Fig. 1. von Békésy's cochlear travelling wave. (A) A travelling wave on the basilar membrane at 200 Hz. The wave envelope (the maximum displacement over a cycle) is indicated by the dotted line, with solid lines showing four wave shapes at different phase angles. (B) The displacement phase of the basilar membrane is shown by the solid line, indicating a phase lag exceeding that of a simple resonator (von Békésy, 1960).

discrimination (Horridge, 1960). Further investigations testing the presence of a 'place principle' in invertebrates then showed that discrete groups of mechanosensory cells from Müller's organ convey different frequency information and attach at different locations to the TM (Michelsen, 1968, 1971; Miller, 1977; Römer, 1976). The logical, but difficult, step forward required establishing a direct relation between the vibrational patterns of the TM and the attachment loci of the mechanosensory cells. This task was first undertaken by Michelsen (1971), using laser holography as a technique and membrane-drum resonance theory as a conceptual background. Data were mostly gathered in isolated ear preparations yielding amplitude and phase information on membrane deflections that coincided with theoretical deflection modes of a circular isotropic drum. Thus, a correspondence was established between the frequency response of the four types of mechanoreceptors, the resonant frequencies of Müller's organ and the mechanical response of the TM. The evidence pointed then to a process in which the locust TM undergoes different resonant modes at different frequencies. The locations of maximal membrane displacements – the antinodes – were seen to vary as a function of the frequency driving the mechanical system, and correspond to the attachment points of mechanoreceptor clusters. This was the place principle applied to the locust ear.

Despite the careful considerations given at the time, the evidence may not have been conclusive. Numerous valid cautionary statements were expressed in the original work (Michelsen, 1971) and merit mention here. First and foremost was the acknowledgement that the TM was assumed to behave as an ideal circular membrane. It was then plainly recognised that "it is obvious that the entire tympanum is very far from being homogeneous and that the thin part of the membrane […] is not circular" (Michelsen, 1971, p. 80). Although good agreement was obtained between the numerical values of the predicted resonance frequencies and those measured by laser holography and a capacitance electrode, resonance frequencies were observed to vary by 10–15%, depending on the desiccation level of the isolated preparation. The data also provided evidence that there is much uncertainty in the actual position of the nodes and anti-nodes on the TM. It was repeatedly observed that: "the most surprising deviation from theory is that the spatial position of the centre of vibration is not constant" (Michelsen, 1971, p. 80). The extent of, and possible reasons for, discrepancy – and agreement – between Michelsen's results and those of the present study will be more thoroughly presented in the discussion.

Here, the vibration characteristics of the locust's tympanal system are examined using intact, live animals, and with non-invasive methods. The sound levels used to drive the tympanal system are of mild intensities, i.e. 60 dB SPL (Sound Pressure Level, 0 db relative to 20 μPa) or about 12–18 dB above neural thresholds, and are most unlikely to elicit non-linearities associated with high-intensity stimuli. The remote sensing method used for vibration measurement is microscanning laser Doppler vibrometry, a method allowing the coherent and load-free measurement of the vibration velocities of the entire surface area of the locust's TM, over a broad range of driving frequencies (1–30 kHz) and small amplitudes (down to 10 pm) (Robert and Lewin, 1998). This study measures in spatio-temporal detail the vibrational deflections of the locust's TM. Travelling waves are identified and their propagation paths are described in three-dimensions for different stimulus frequencies. The temporal and spatial characteristics of the waves are compared and discussed in relation to previous works, including those on mammalian auditory systems.

Materials and methods

Animals

Experiments were performed using adult male and female *S. gregaria* Forskål, with a total of ten animals used. Some additional experiments were also conducted on male and female *L. migratoria* L. to provide a comparison against the results found here and in previous work. The animals were supplied by Blades Biological (Cowden, UK), and kept in standard conditions. For the mechanical measurements the animal's wings were cut back to allow direct optical access to the tympanal organs. The experimental protocol ensured that all insects survived the experiment. While measured, the animals were firmly attached, ventrum down, to a horizontal brass bar (5 mm wide, 1 mm thick and 60 mm long) using BLU-TACK (Bostik-Findley, Stafford, UK). The brass bar was connected to a metal rod (150 mm long, 8 mm diameter) via a thumbscrew, allowing the animal to be rotated and tilted into the required position. Only one ear was examined per animal. The animal was orientated such that the measuring laser

Doppler vibrometer could scan the entire TM and that the tympanum was perpendicular to the direction of sound wave propagation. All experiments were carried out on a vibration isolation table (TMC 784-443-12R; Technical Manufacturing Corp., Peabody, MA, USA) at room temperature (24–26°C) and relative humidity of 40–62%. The vibration isolation table with the animal and the laser vibrometry measurement head were located in an acoustic isolation booth (IAC series 1204A; internal dimensions – length 4.50 m, width 2.25 m, height 1.98 m; Industrial Acoustics, Bronx, NY, USA).

Mechanical and acoustic measurements

Tympanal vibrations were examined in response to acoustic stimulation with wideband (chirp) signals of frequency range 1–30 kHz. The vibrations were analysed by simultaneous recording of the vibration velocity, **U**, of the TM, and the SPL adjacent to the tympanum. **U** was measured using a microscanning laser Doppler vibrometer (Polytec PSV-300-F; Waldbronn, Germany) with an OFV-056 scanning head fitted with a close-up attachment. This allowed the laser spot (~5 μm diameter) to be positioned with an accuracy of ~1 μm. Measurements across the entire TM could be taken without re-adjusting the position of any component in the experiment. The laser spot position was monitored *via* a live video feed to the vibrometer's controlling computer. The surface area of the TM could thus be scanned with high spatial accuracy, each scanning lattice comprising hundreds of measurements points (Fig. 2C). The laser vibrometer thus allowed accurate measurement of the topography of tympanal motion in the amplitude, time and frequency domains, in a contact-free way and without requiring the use of a reflective medium.

The acoustic signals were generated by the PSV 300 internal data acquisition board (National Instruments PCI-4451; Austin, TX, USA), amplified (Sony Amplifier Model TA-FE570; Tokyo, Japan) and passed to a loudspeaker (ESS AMT-1; ESS Laboratory Inc., Sacramento, CA, USA) positioned 300 mm from the animal. Thus, for the relevant frequency range (3–30 kHz), the animal was in the far-field of the sound source. SPL was measured using a 1/8 inch (3.2 mm) precision pressure microphone (Bruel & Kjaer, 4138; Nærum, Denmark) and preamplifier (Bruel & Kjaer, 2633). The microphone has a linear response in the measured frequency range. The microphone's sensitivity was calibrated using a Bruel & Kjaer sound level calibrator (4231, calibration at 1 kHz, 94 dB SPL). The microphone was positioned 10 mm from the tympanum, with its diaphragm parallel to the sound direction, thus maximizing the response. A calibrated stimulus sound level, at the tympanum, of 20 mPa (60 dB SPL) was used throughout these experiments. Computer correction of the stimulus acoustic signals ensured that their amplitude was kept to a constant level (60 dB SPL) across the complete range of frequencies (1–30 kHz). The incident sound spectrum, as measured by the reference microphone, was measured in signal voltage and inverted with respect to amplitude. The resulting voltage-frequency function was fed back to the waveform generator to create another, corrected spectrum to flatten the frequency composition of the stimulus at the position of the reference microphone (Fig. 3A).

Evaluation of data

The analysis of the membrane velocity, **U**, and SPL was carried out by the vibrometer's control PC. The signals were simultaneously sampled at 102.4 kHz. Sets of 25 data windows of 80 ms duration were acquired and averaged for each point across the TM. Using an FFT (Fast Fourier Transform) with a rectangular window, a frequency spectrum was produced for each signal with a resolution of 12.5 Hz. The laser and microphone signals were then used to calculate different quantities, such as gain and phase responses. By combining the results from all the points scanned across the TM, oscillation profiles and animations of tympanal deflections were generated for specific frequencies. In this work we calculated the transfer function (H_1) of the membrane velocity **U** (ms^{-1}) to reference sound level SPL (Pa), to produce the amplitude gain and the phase response of the system at different frequencies. Therefore,

$$H_1 = G_{ab}(f) / G_{aa}(f) , \quad (1)$$

where, $G_{ab}(f)$ is the cross-spectrum of the velocity signal and reference signal, and $G_{aa}(f)$ is the auto-spectrum of the reference signal. The magnitude-squared coherence (C) between the vibrometer and microphone signals were also computed for each data point to assess data quality for the entire data set, given by

$$C = G_{ab}(f)\, G_{ba}(f) / G_{aa}(f)\, G_{bb}(f) , \quad (2)$$

where, $G_{ba}(f)$ is the cross-spectrum of the reference signal and velocity signal, and $G_{bb}(f)$ is the auto-spectrum of the velocity signal.

Data were considered of sufficient quality when coherence exceeded 85%. Typical coherence maps are shown in Fig. 2D, illustrating high data reliability over the entire extent of the tympanal surface area.

Characterisation of travelling waves – the criteria

Characterisation of travelling waves was carried out as part of the analysis of the tympanum's vibrations. Unlike standing waves, such as the vibrations of a violin string, travelling waves do not remain constant in position but move with time, so that the vibrations vary with both distance, x, and time, t. In the cochlea, this wave propagation induces characteristic mechanical signatures into the mechanics of the basilar membrane that are used here as operational criteria to characterize the travelling waves in the locust ear. The three main response characteristics of the basilar membrane introduced by the travelling wave are as follows (von Békésy, 1960; Robles and Ruggero, 2001).

(1) Displacement shows increasing phase lag along the propagating medium. At a given location the motion of the medium increasingly lags the motion of its point of origin. In the cochlea, this increasing delay with position is also a function of stimulus frequency because the basilar membrane

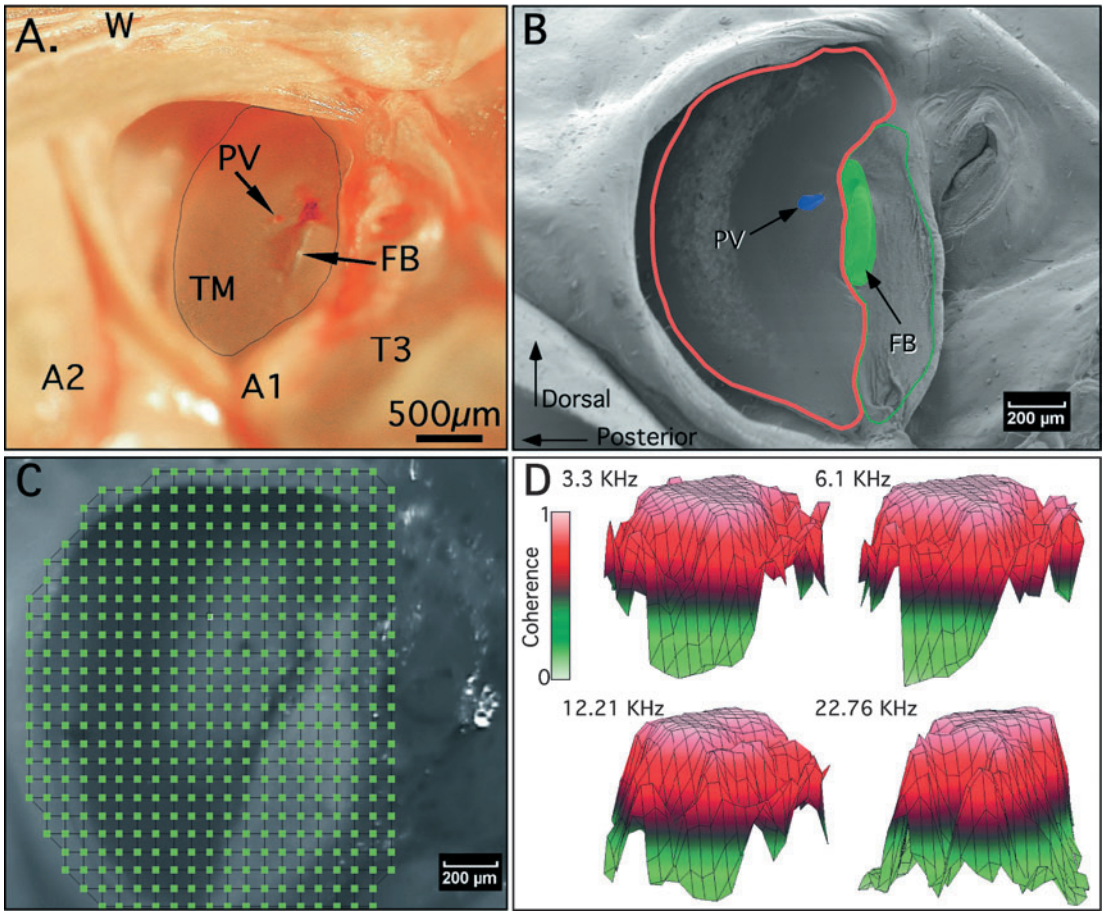

Fig. 2. Measuring tympanal vibrations in the locust *S. gregaria*. (A) Anatomical position of the ear on the abdomen of the locust. TM, tympanal membrane; W, wing; A1, first abdominal segment; A2, second abdominal segment; T3, third thoracic segment. (B) SEM of locust ear. Thin membrane outlined in red, thick membrane outlined in green; PV, insertion point of the pyriform vesicle (high frequency mechanoreceptors, highlighted in blue); FB, insertion point of the folded body (low and mid frequency mechanoreceptors, highlighted in green). (C) Capture of the video image from the laser Doppler vibrometer illustrating the viewing angle of the TM during measurements and the lattice of laser scanning points (N=488 points; scanning mesh size: 70 μm, dot positioning accuracy: ~1 μm). (D) Coherence maps of the tympanal vibrations at 3.3, 6.1, 12.21, 22.76 kHz. For each scan, coherent data (>85%) could be taken on ~350 data points across the entire surface of the TM. Because only the tympanum moves in a coherent way with sound, coherence drops beyond its edge.

translates frequency into space. In the frequency domain, the delay manifests itself as a phase accumulation at high frequencies, which exceeds the high frequency phase-lag expected for simple resonators.

(2) Displacement magnitudes have an asymmetric envelope around the point of interest, where the wave is seen to compress. At a given location on the propagating medium the leading slope of the envelope is steeper than the trailing slope.

(3) The cochlear travelling wave results from the mechanical characteristics of the propagating medium (mass, stiffness, damping) and, in that sense, is passive.

Travelling waves can be both identified and characterized if the phase responses at closely spaced locations are compared (Robles and Ruggero, 2001). The wavelength and velocity of the travelling wave is then calculated according to the following equations (Robles and Ruggero, 2001):

$$\delta_t = \delta_\phi / 2\pi f\,, \tag{3}$$

$$\mathbf{V}_{wave} = \delta_x / \delta_t\,, \tag{4}$$

$$L_{wave} = 2\pi\delta_x / \delta_\phi\,, \tag{5}$$

where f is wave frequency, δ_ϕ is phase difference between the two locations, δ_t is the travel time, δ_x is the distance travelled, $\mathbf{V}_{wave}$ is wave velocity and L_{wave} is wavelength.

Results

The locust tympanal membrane (TM)

The auditory organs of the locust are situated on each side of the first abdominal segment (Fig. 2A). In the locust *S. gregaria*, the tympanal membrane (TM) can be recognised by its shiny and semitransparent appearance. Two particular landmarks can be readily identified by light photography: the pyriform vesicle (PV), which is the site of attachment of the high-frequency mechanoreceptors, the ‘d’ type receptors (Gray, 1960); and the folded body, a region of thicker and less

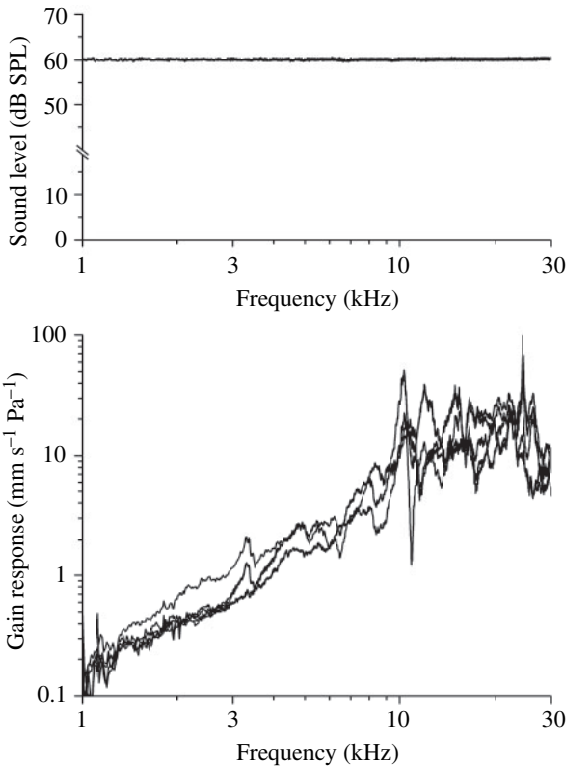

Fig. 3. Acoustic stimulus and mechanical response at the attachment point of the pyriform vesicle (PV) on the TM. (A) Amplitude frequency spectrum of the incident acoustic stimulus; the reference signal. Over the frequency range used the spectrum is flat within ±0.4 dB. (B) Response gain at the PV (blue dot in Fig. 2B) for five different insects. The response gain is the transfer function between the measured mechanical vibrations and the measured acoustic incident stimulus (see Materials and methods).

compliant cuticle, to which the low frequency-receptors ('a', 'b', and 'c' types) project. Previous investigations have revealed that the TM of different locust and grasshopper species is not a homogeneous structure (Michelsen, 1971; Stephen and Bennet-Clark, 1982; Breckow and Sippel, 1985; Jacobs et al., 1999). As highlighted in Fig. 2B, the TM is composed of a thin, posterior part (encircled in red), and a thicker, anterior part (encircled in green).

TM vibrations: LDV scans

The TM of the locust *S. gregaria* is completely accessible to non-contact mechanical measurements by laser Doppler vibrometry. Hundreds of measurement points were selected and repeatedly measured during controlled acoustic stimulation (Fig. 2C). The quality of each measurement point was evaluated by estimating the magnitude-squared coherence (Equation 2; see Materials and methods) for different frequency bands (Fig. 2D). Each single measurement point provides coherent (thus reliable) amplitude and phase data on the mechanical response of the membrane at that point. The mechanical response of the attachment point of the PV to the TM (blue dot in Fig. 2B) was measured in response to broadband (1–30 kHz) iso-intensity stimulation and evaluated as an amplitude frequency spectrum (Fig. 3B). The amplitude response, displayed as the response gain (Equation 1), shows a steady increase across the frequency range. For higher frequencies, in the range from 10 to 30 kHz, the amplitude frequency spectrum indicates larger response fluctuations in the mechanical response, an effect most probably related to some variation in local diffractive acoustics around the locust's body (Miller, 1977).

The entire TM of *S. gregaria* was scanned to determine its response at a variety of frequencies. In Fig. 4, examples of scans of the entire membrane are presented. To ease orientation, a video capture of the tympanum (Fig. 4A, left panel) and of the associated topographically calibrated scan data (Fig. 4A, right panel) are shown. The response gain of the membrane was evaluated for four different frequencies, and shown for each frequency, at four different phase angles, 90° apart, in the cycle of that frequency. The scans reveal that, at each of the different frequencies, travelling waves are generated on the TM. For each frequency the tympanal deflections do not stay in position, but travel across the tympanum from posterior to anterior (from left to right in Fig. 4B), starting at the edge of the thin membrane. At 3.3 kHz the wave travels across the thin membrane, moving towards a focus point located at the folded body (see Movie 1 in supplementary material). At 6.1 kHz the wave propagates across the thin membrane along the same line as at 3.3 kHz, but dissipates (ends) at the locations of the elevated process and styliform body. At 12.21 kHz and 22.76 kHz the wave takes a semi-concentric shape at the location of its initiation, on the thin membrane. As the wave travels across the tympanum (Fig. 4B, see 22.76 kHz, phase angles 90°, 180°, 270°, and see Movie 2 in supplementary material) the advancing wave front converges towards a single point, creating a focal point of vibration. This location corresponds to the point of attachment of the PV to the TM. The focusing of the travelling waves to different attachment sites of the mechanoreceptors at different frequencies corresponds to those of previous mechanical and physiological studies (Michelsen, 1971; Jacobs et al., 1999).

Interestingly, the propagation of the travelling wave does not depend on the angle of incidence of sound impinging on the TM. Irrespective of the angle of stimulation (i.e. the relative angle between loudspeaker and tympanum), the waves always propagated in one direction (from the thin membrane to the thick membrane), converging on identified mechanoreceptive attachment sites (data not shown).

The characterisation of travelling waves

The mechanical deflection shapes observed on the locust TM present the three key characteristics of cochlear travelling waves.

Criterion 1: the phase response across the locust's TM shows an increasing phase lag as a function of stimulus frequency (Fig. 5). This phase lag is substantial, exceeding the phase lag expected for the velocity response of a simple resonator

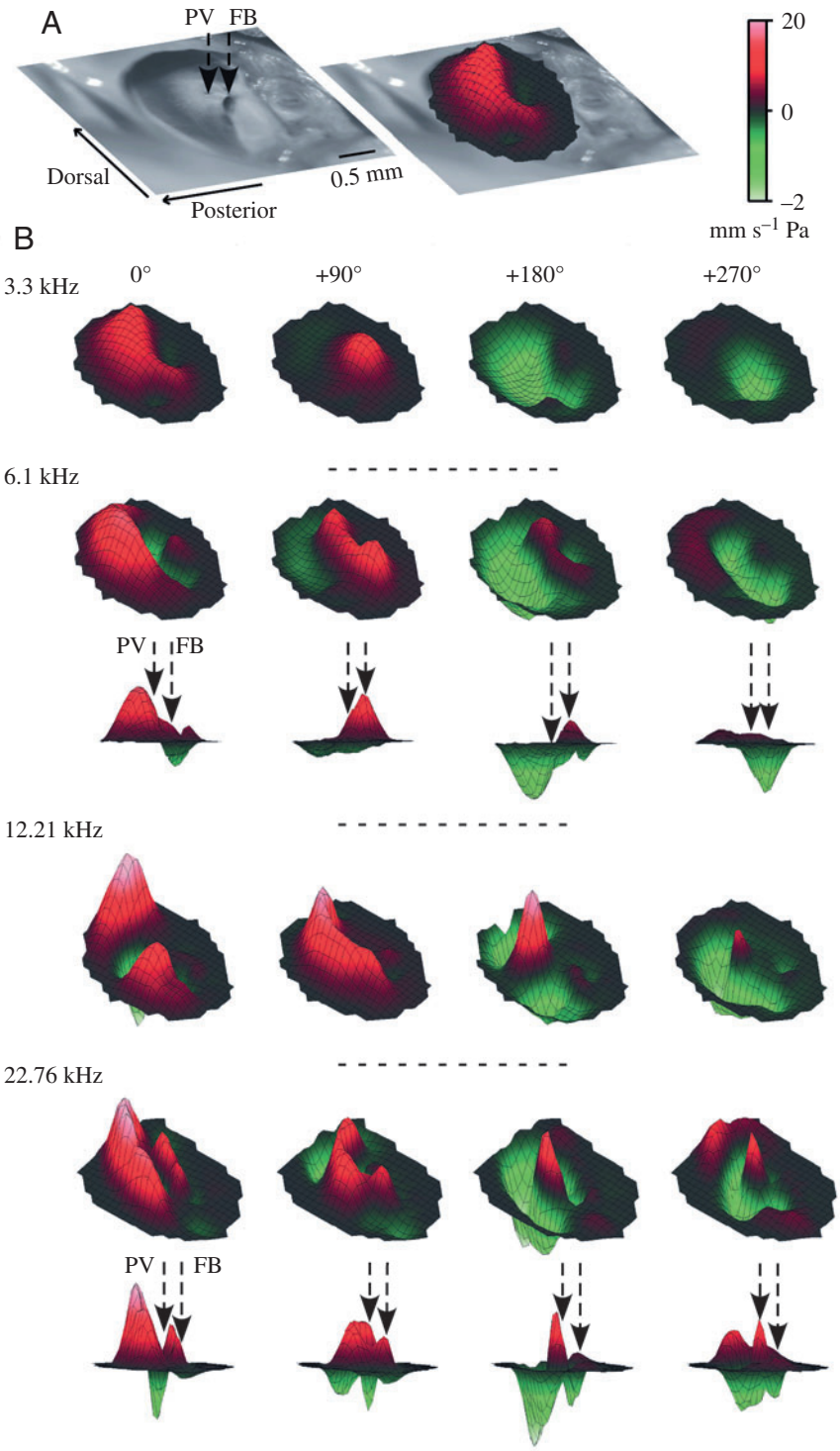

Fig. 4. Area scan and deflection shapes of TM in *S. gregaria*. (A) Orientation image relating tympanal topography (left image) to the position of the scanning lattice (right image). Vertical arrows depict the position of the pyriform vesicle (PV) and folded body (FB). (B) Area scans of tympanal deflections for four different frequencies. The deflections are shown each time for four different phases along the oscillation cycle (see also movies in supplementary materials). For 6.1 kHz, and 22.76 kHz, deflections are additionally shown as profiles, as if looking at the tympanum from its side. Red indicates positive velocities (or outward tympanal deflections), and green negative velocities (or inward tympanal deflections). The scale for deflection velocity magnitudes applies to all scans.

(maximum of –90° at frequencies above resonance). Lag increases as a function of frequency; at higher frequencies, such as 30 kHz, the phase lag reaches nearly 900° (2.5 cycles).

Criterion 2: the magnitudes of TM displacement show an asymmetric envelope around the point of the maximal deflection. This point is also the location where the wave is seen to compress, before dying off. Wave asymmetry was evaluated as the response gain (**U**/SPL) along a transect line across the membrane (Fig. 6A) for five different frequencies (Fig. 6B–F). The envelope of the wave in motion across the tympanum becomes apparent when the response is displayed for every 10° of phase. As expected, the envelope of the travelling wave varies with the driving frequency. At 3.3 kHz (Fig. 6B) the wave is asymmetrical about a point 1.2 to 1.4 mm along the transect. This location coincides with the insertion point (the elevated process) of low frequency mechanoreceptors. At 6.05 kHz (Fig. 6C), the wave is asymmetrical about a point 0.8 to 1.0 mm along the transect. Maximal deflection does not directly correspond to mechanoreceptor location, which, in this case, is not completely aligned with the chosen transect. At 12.1 kHz (Fig. 6D), the wave is sharply asymmetrical about a point 0.9–1.0 mm along the transect. The location of maximal amplitude corresponds to the insertion point of the PV to the TM. Direct comparison with the deflection envelope at lower frequencies (eg. Fig. 6B,C) shows that higher frequencies do not elicit motion past 1.1–1.2 mm along the transect. Notably, past the point of maximal deflection (0.9–1.0 mm along the transect, Fig. 6D) the slope of the envelope is very steep, resulting in little motion of the thick part of the membrane, the part to which low frequency receptors attach. The energy of the wave is thus maximally focussed, in a frequency specific manner, to the relevant mechanoreceptors. At both 22.6 kHz (Fig. 6E) and 26 kHz (Fig. 6F) the wave is sharply asymmetrical 1.0 mm along the transect. For both frequencies, the location of maximal deflection corresponds with the position of high frequency mechanoreceptors. Notably, these high frequency travelling waves have shorter wavelength and thus undergo several cycles along the span of the membrane they propagate across. Again, nearly all of the membrane motion elicited by the wave is focussed at the

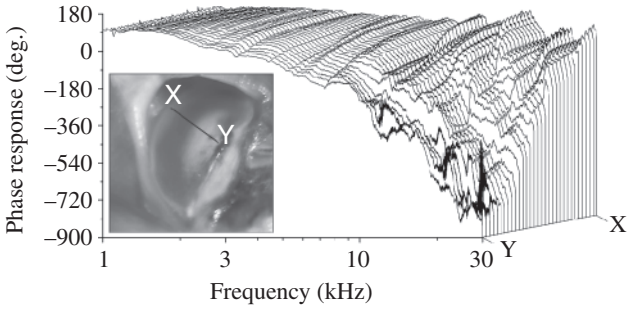

Fig. 5. Phase response of the TM along a line of transect. The inset shows the exact extent and orientation of the transect. The phase response shows an increasing lag with both frequency and distance along the transect. The phase lag increases to –900°, substantially greater than that of the velocity response of a simple resonator (–90°).

1 mm location, with very little motion of the thick membrane (past 1.1 mm along the transect). Thus, the energy of the travelling wave is compressed into the maximal displacement at the PV, and efficiently dissipated there, resulting in no further propagation of the high frequency wave to other mechanosensory connection sites (thick membrane).

Criterion 3: Travelling waves result from the mechanical properties of the wave propagating substrate (mass, stiffness, damping). In that sense they are not related to the physiological mechanisms linked to the process of mechanoreception and transduction. In locusts, scanning measurements indicate that the pattern of the travelling waves in dead animals (Fig. 7) is not distinguishable from that of live specimens (Fig. 4B). This is true for both lower frequencies (6.1 kHz; Fig. 7) and higher frequencies (16.24 kHz; Fig. 7).

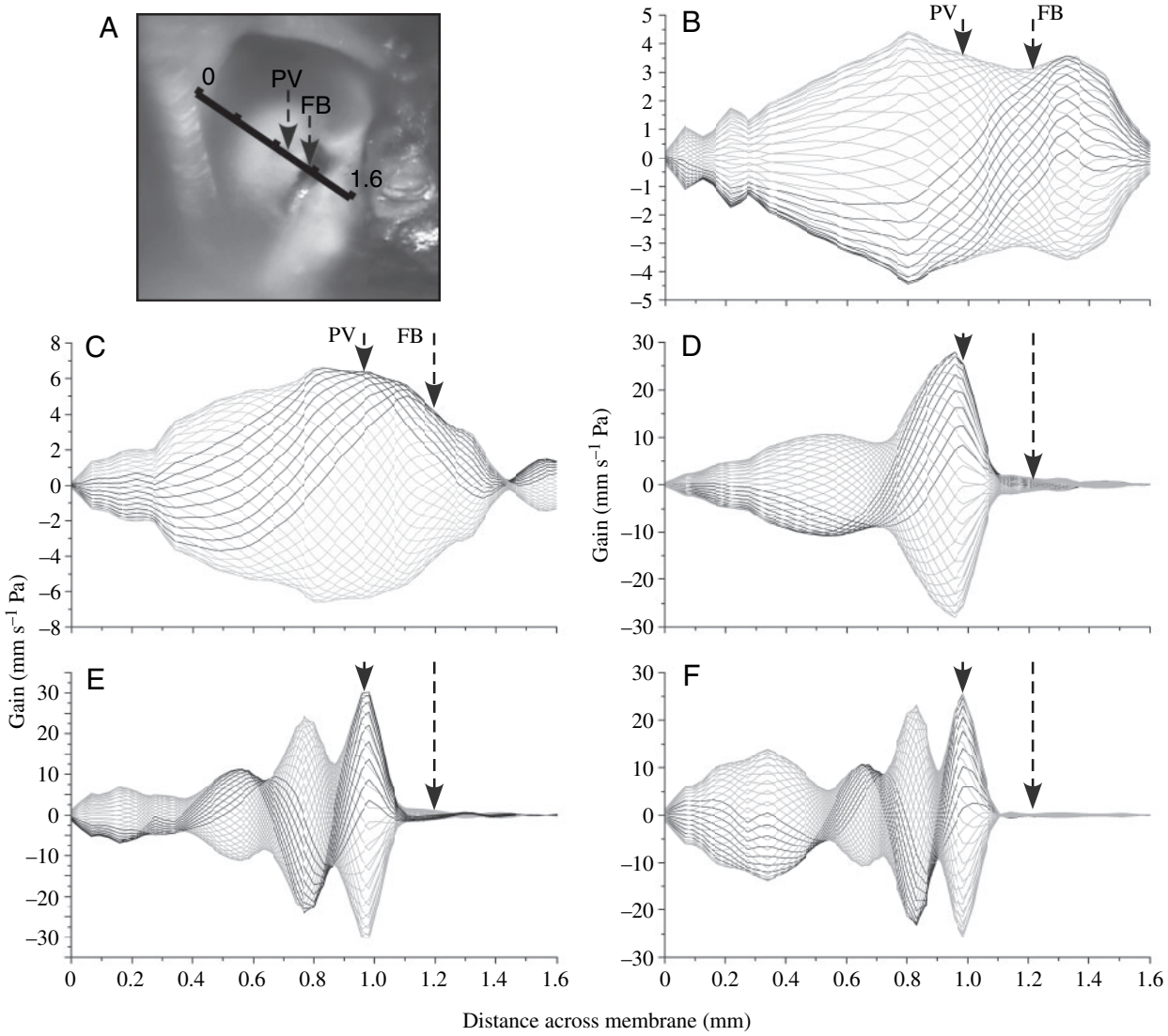

Fig. 6. Envelopes of mechanical deflections across the TM along transect lines for different driving frequencies. (A) The position along the transect line is given with a calibrated scale. This scale constitutes the *x*-axis in panels (B–F). The deflection envelopes are constructed by displaying the instantaneous deflection velocities along the transect for a series of phases in the full oscillation cycle. For each frequency, deflections are shown for phase increments of 90°. Vertical arrows depict the position of the pyriform vesicle (PV) and folded body (FB) along the transect line. Driving frequencies: (B) 3.3 kHz; (C) 6.05 kHz; (D) 12.1 kHz; (E) 22.6 kHz;(F) 26 kHz. High frequencies undergo several oscillation cycles across the span of the transect.

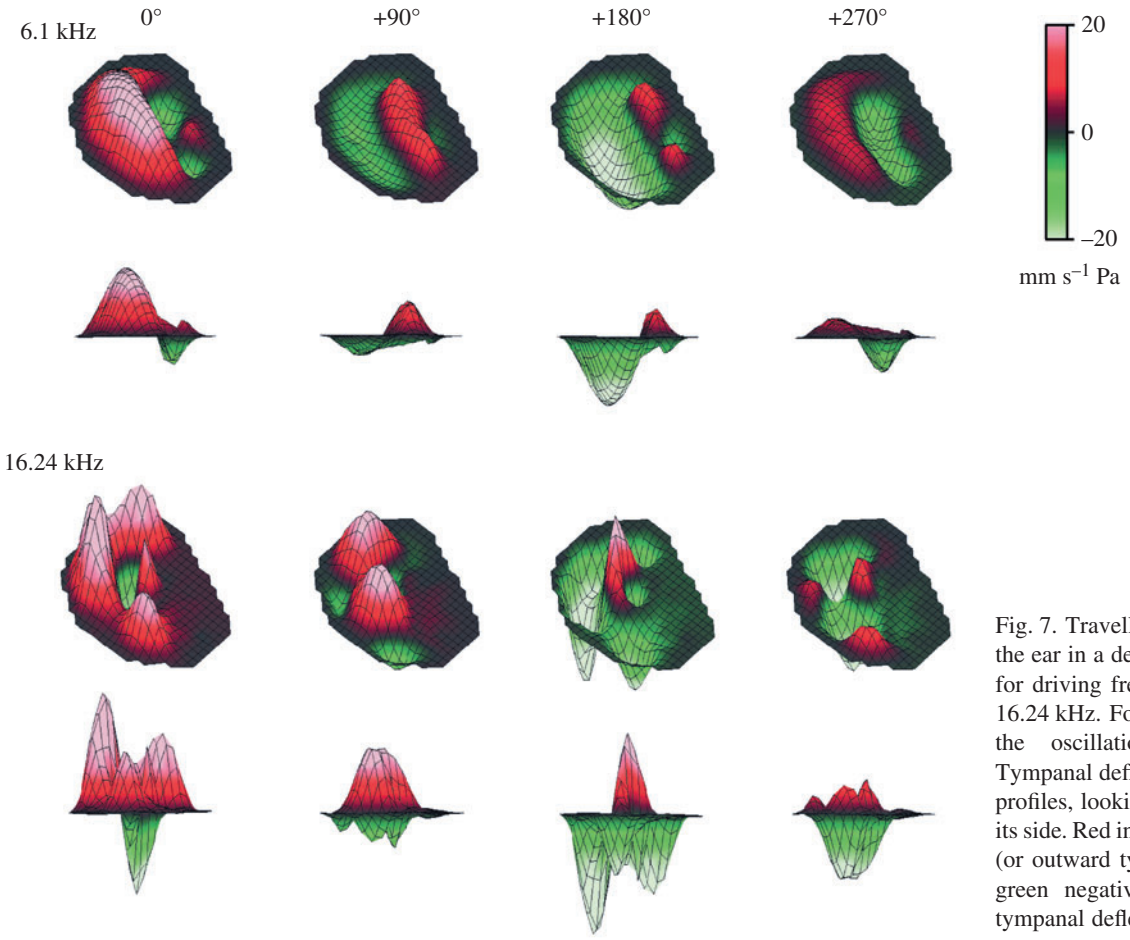

Fig. 7. Travelling wave phase steps for the ear in a dead animal. Data is shown for driving frequencies of 6.1 kHz and 16.24 kHz. Four different phases along the oscillation cycle are shown. Tympanal deflections are also shown as profiles, looking at the tympanum from its side. Red indicates positive velocities (or outward tympanal deflections), and green negative velocities (or inward tympanal deflections).

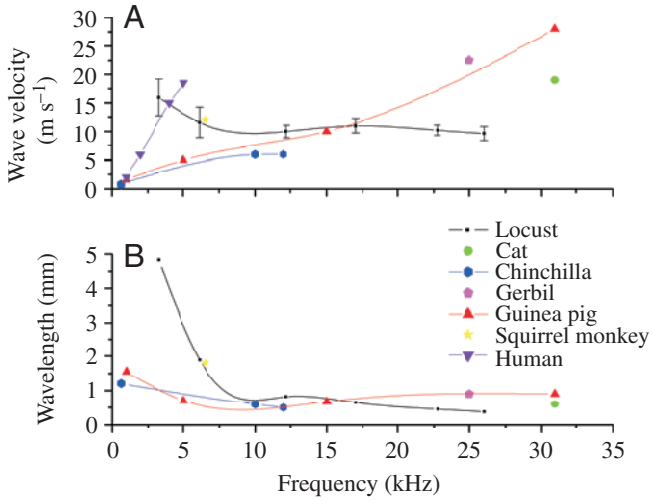

Fig. 8. Comparison of travelling wave characteristics between the locust and several mammalian species. (A) Wave velocity. (B) Wavelength. Previously reported values from: cat, Cooper and Rhode (1992); chinchilla, Narayan and Ruggero (2000), Rhode and Recio (2000), Cooper and Rhode (1996); gerbil, Olson (1999); Guinea pig, Cooper and Rhode (1992), Russell and Nilsen (1997), Kohllöffel (1972), Cooper and Rhode (1996); squirrel monkey, Rhode (1971); human, Serbetcioglu and Parker (1999). Wave velocity values for humans were not directly obtained from the basilar membrane, but calculated from auditory brainstem responses.

The travelling wave's length and propagation velocity

The wavelengths and wave velocities for the locust's TM were calculated using Equations 3, 4 and 5. Wavelengths and wave velocities are reported in Fig. 8, along with results for cochlear sites in several mammalian species. In the locust, for example, it was found that for 60 dB SPL stimulus at 12.21 kHz, the phase shift calculated over a transect length of 1.1 mm amounts to 1.33 periods. This results in an average wavelength of 0.82 mm (S.D.=±5×10^{-5}, N=10) and an average wave velocity of 9.99 ms^{-1} (S.D.=±1.11, N=10). Wave velocity in the locust is somewhat higher at lower (<10 kHz) than at higher frequencies (up to 30 kHz). In effect, wave velocity ranges from 9.6 to 15.9 ms^{-1}, values that are in the same order of magnitude as those of mammalian species (Fig. 8). In the locust's low frequency range, length of the travelling wave is relatively long, displaying a top value around 5 mm, exceeding all those reported for mammalian species (Fig. 8). At higher frequencies, wavelengths in the order of 1 mm were measured, a length similar to that of mammals for that frequency range.

Travelling waves in Locusta migratoria

Tympanal vibrations were also investigated in *L. migratoria* using the same experimental procedure as for *S. gregaria*. In *L. migratoria*, a flap of cuticle partly obscures the anterior

aspect of the TM. This flap was not removed to respect the protocol of intact, non-invasive measurements. The deflection shapes from the TMs of both locust species display the propagation of a travelling wave (Fig. 9). For *L. migratoria*, the 3.4 kHz wave travels across the thin membrane, as seen for *S. gregaria*, before disappearing out of view behind the cuticle flap. It is presumed that the wave progresses to the area of the folded body, the site of low frequency reception. At 6.1 kHz, the wave crosses the thin membrane in a way identical to that described before (Fig. 4) and can be seen dissipating at the location of the elevated process and styliform body (Fig. 9). At 12.6 kHz and 22.64 kHz the wave appears semi-concentric again, and as with *S. gregaria*, converging as it propagates towards the PV. In this case, the average wavelength and wave velocity at a frequency of 22.64 kHz were found to be 0.67 mm (S.D.=±1.4×10^{-4}, N=5), and 15.15 ms^{-1} (S.D.=±3.19, N=5), respectively. The values are similar to those found in *S. gregaria*.

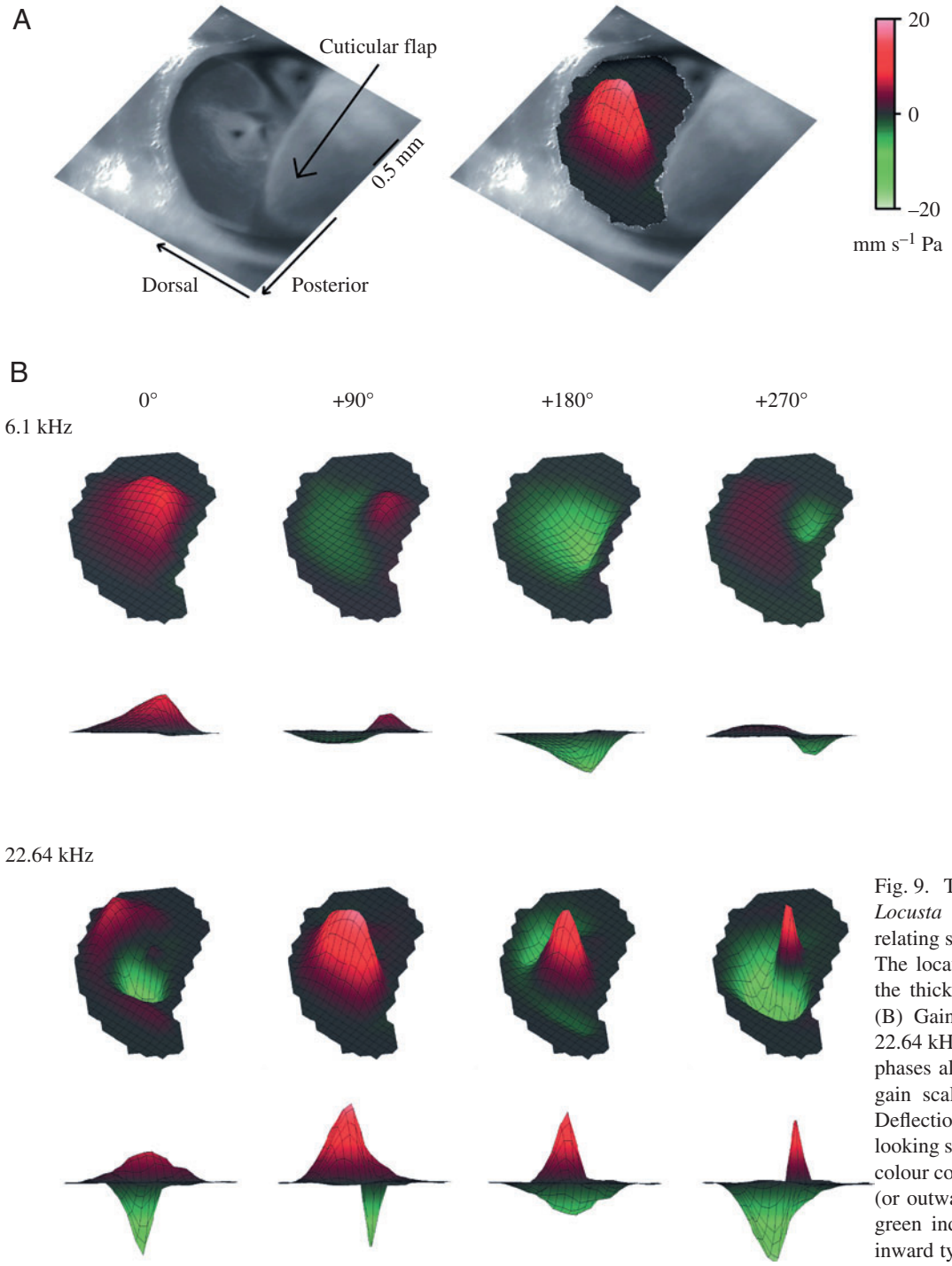

Fig. 9. Travelling wave observed in *Locusta migratoria*. (A) An image relating scan data to tympanal anatomy. The location of the cuticular flap over the thick part of the TM is indicated. (B) Gains across the TM at 6.1 and 22.64 kHz shown for four different phases along the oscillation cycle. The gain scale applies to both A and B. Deflections are also shown as profiles, looking sideways at the tympanum. Red colour code indicates positive velocities (or outward tympanal deflections), and green indicates negative velocities (or inward tympanal deflections).

Discussion

In 1971, Michelsen published a substantial work, a series of three papers, relating the motion of the locust's TM to the frequency characteristics of the sensory neurons in Müller's organ. This work provided the formal basis for the 'place principle' as applied to locust hearing. In brief, tympanal mechanics and frequency selectivity were portrayed as follows. (1) The thin and thick parts of the TM are distinct mechanical entities (Michelsen, 1971, p. 63), each endowed with distinct physical characteristics, such as thickness, mass distribution, stiffness and anisotropy. (2) The observed vibrational patterns varied across the entire TM in a frequency specific manner, with high frequency and low frequency stimulation resulting, respectively, in prominent motions of the thin and thick parts of the membrane. (3) Mechanical deflections were interpreted using the symmetric vibration modes of circular homogenous membranes predicted by theory. Importantly, tympanal motions were expected to display nodal lines (immobile zones of nil deflection), the locations thereof being predictable for specific driving frequencies. (4) Distinct tympanal areas were thus reported to undergo maximal vibrations for specific frequencies and were topographically linked to the attachment locations of mechanoreceptor cell clusters known to report frequency-specific information (Horridge, 1960; Michelsen, 1971).

The findings of the present study concur with those of the 1971 study on several aspects of tympanal mechanics, but not, crucially, on the mechanical basis of frequency discrimination in the locust. Our observations on tympanal structures corroborate point 1 listed above. The distribution of maximal tympanal deflections across different areas of TM is also observed, and generally is in accord with point 2 above. Addressing point 3, our study fails to confirm Michelsen's report of the presence of nodal lines (figs 13–15 in Michelsen, 1971) in the mechanical deflections of the TM. Importantly, the presence of nodal lines is characteristic to standing waves and constituted the basis for identifying modes of deflection using drum theory. These modes were then used to attribute phase relationships to distinct tympanal areas and compare them with data gathered with a capacitance electrode. Frequency-specific locations of large deflection were then described, and said to coincide with tympanal locations. Incidentally, Michelsen also observed that the location of maximal deflection (the centre of vibration) on the thin membrane moved across the drum surface area (Michelsen, 1971, p. 80). In the logic of drum theory, the centre of vibration ought not to wander. This observation seems to coincide with the phenomenology of the travelling wave reported here. Supporting the general message of point 4, the present study shows that different tympanal areas undergo different vibrational regimes, but through a mechanical process that is not related to drum resonance.

Several issues related to methodology may explain the similarities and the discrepancies between the results of Michelsen's study and the present one. In the 1971 study, the locust's auditory mechanics was investigated using two different measurement techniques; laser holography and a capacitance electrode. Fundamentally, the complete characterisation of the mechanical response of a vibrating object requires characterisation of three basic variables: the location of vibration, its amplitude, and its time course. It was plainly recognised then that each technique has its pros and cons: laser holography provided information on two variables, the static topography of membrane deflections and their relative amplitudes. Crucially, laser holography did not provide phase information (Michelsen, 1971, p. 70). The capacitance electrode method, in turn, provided some topographical information and quite accurate time domain information, but yielded unreliable amplitude data (Michelsen, 1971, p. 70). These methodological shortcomings constrained data interpretation, requiring theoretical support to make sense of the observed mechanical behaviour. Of the two theories available at the time, the resonance theory and the travelling wave theory, the former was favoured to provide the background against which to evaluate the data (Michelsen, 1971, p. 64). The travelling wave theory (von Békésy, 1969) was mentioned but not considered as an alternative explanation.

Tympanal deflections measured by laser holography were interpreted using the motions theoretically expected from drum resonances. It was assumed that the TM would behave like a circular homogenous drum, although it was recognised at the time that the membrane was neither circular nor homogeneous (Michelsen, 1971, p. 66). Different modes of drum resonance with central symmetry were used to explain the observed concentric rings of amplitude maxima and minima (figs 13–15 in Michelsen, 1971). Laser holography has limited sensitivity, dynamic range and temporal resolution. In effect, that technique produced static contour images of high amplitude tympanal deflections. Thus the data did not contain information of membrane motion over the entire deflection cycle resulting from incident acoustic energy. What were interpreted as the transitions between antinodes and nodal lines can now be regarded as the crests of converging travelling waves. As expected, high frequency (12 kHz and above, Fig. 6B,C) stimulation generates several travelling wave peaks across the tympanum, while low frequencies do not (Fig. 6E,F). Variation of multiple peaks was observed, although in a static manner, in the former study (fig. 15 in Michelsen, 1971).

Another possible source of uncertainty may lie in the intensity of the acoustic stimuli used. The acoustic stimuli used to drive the tympanal system were delivered at high sound pressure levels (96–112 dB SPL), a necessity imposed by the relative insensitivity of the techniques. The use of high SPL raises the possibility that the tympanal system may have been driven in the non-linear range of its mechanical response. The system was deemed to obey Hooke's law over a narrow range of amplitudes (50–100 μm) (Michelsen, 1971, p. 72), and there is no indication of Young's modulus in the sub-micrometre range (fig. 7 in Michelsen, 1971). This point may bear some importance since measurements at biologically relevant sound

pressure levels (60 dB SPL) yield membrane motions on different membrane locations with amplitudes between 1 and 10 nanometres. Motions at this length scale have also been reported in previous studies on insect hearing organs (Göpfert and Robert, 2000). On a linear scale, the observed displacement amplitudes are smaller by three to four orders of magnitude (60–80 dB), leaving the possibility open that the modes of tympanal motion differ between moderate (60 dB SPL) and high (104 dB SPL) sound pressure levels.

Two other investigations have described the mechanical vibrations of the locust tympanum in terms of resonances with different modes (Stephen and Bennet-Clark, 1982; Breckow and Sippel, 1985). Although capable of greater sensitivity, the methods used then, e.g. stroboscopy, still provided a relatively poor sensitivity (1 μm) (Breckow and Sippel, 1985). The acoustic stimulation required for reliable measurements was also at very high sound pressure levels (100–112 dB SPL). An analysis of the mass and thickness distribution of the TM was undertaken by Stephen and Bennet-Clark (1982), in a study that established that important mechanical interactions take place between the tympanal mechanics and Müller's organ. As in other studies, the tympanal system had to be removed from the animal, and the surrounding cuticle was sometimes removed to gain access to the tympanum (depending on species). At this time it was again assumed that the tympanal system would behave linearly up to such sound pressures, and thus mechanical displacements at mid-range sound levels (60 dB SPL) were extrapolated. Most recently, Jacobs et al. (1999) directly correlated the soma position, the attachment site of the dendrite and the physiologies of individual mechanosensory neurons using intracellular recordings and neuroanatomical evidence from cell-specific neurobiotin staining. Using *S. gregaria*, this work established a solid link between neural sensitivity and mechanoreceptor topography for three distinct groups of cell: cells attached to the folded body with responses ranging from 400 to 700 Hz and from 1.5 to 2 kHz, cells attached to the PV with responses from 12 to 25 kHz, and a combination of cells attached to either the elevated process or to the styliform body with responses from 3 to 4 kHz.

It was pointed out earlier that frequency selectivity in locusts seems to rely primarily on the mechanical processing of incoming sound waves (Michelsen, 1971). The present study finds no evidence of change in the shape and propagation of the travelling waves in living and post-mortem animals, pointing only to the sufficiency of the passive mechanical process to generate topographic separation of sound frequencies (Fig. 7). It would, however, be premature to conclude that frequency selectivity is solely brought about by passive mechanical processing in the locust ear. An earlier study has indeed reported the presence of acoustic distortion products in the locust (Kössl and Boyan, 1998), pointing to the possibility of active auditory mechanics in insects, as shown for mosquitoes and fruit flies (Göpfert and Robert, 2001; Göpfert and Robert, 2003). Further studies are required to investigate low-level non-linear mechanics in an insect tympanal ear (J.F.C.W. et al., in preparation).

The comparison between the locust tympanal travelling wave and that of different mammalian species highlights interesting similarities (Fig. 8). Although the geometries and length scales of the two types of auditory systems vastly differ, wave velocities and lengths are similar. For all mammalian species considered, wave velocity tends to increase with the frequency of acoustic stimulation. Velocities can vary, possibly linearly, from 1 ms^{-1} (Chinchilla) to 28 ms^{-1} (Guinea pig). In humans, for example, wave velocity increases quite rapidly from 1 to 5 kHz (data from Serbetcioglu and Parker, 1999). Interestingly, at around 4–5 kHz, wave velocities are very similar for humans and locusts (Fig. 8). A steep increase in wave velocity implies a broader topographic spread of sound frequencies along the cochlea, reflecting the exquisite capacity of frequency discrimination in humans (Rhode and Recio, 2000). By comparison to other species, wave velocity in the locust remains relatively constant over the frequency range representative of the thin part of the tympanum (>10 kHz), but displays higher values for lower frequencies (3–4 kHz). This variation arises because the wave's travel time is a ratio between frequency and phase change (Equation 3). For higher frequencies, as frequency increases, so does the phase difference, whereas at lower frequencies, the phase difference is relatively small (Fig. 5). Therefore for the high range of frequencies the travel time is invariable, but for the low frequency range the travel time changes. In the locust's case both the higher and lower frequencies are measured over a constant distance from membrane edge to PV (higher frequencies) or thick membrane (lower frequencies). Therefore, for higher frequencies the wave's velocity (Equation 4) remains approximately constant, but for lower frequencies it varies as a function of frequency. For the Guinea pig, for instance, phase change appears to be an order of magnitude lower than the frequency change and the analysis of high frequencies is performed over several millimetres of basilar membrane, resulting in a relative increase of wave velocity with frequency. A similar argument can be made for variation in the length of the travelling wave. In the locust, the wavelength is long at lower frequencies because it is a ratio between travel distance and phase change (Equation 5). At lower frequencies, the phase change is small over the distance considered, thus yielding a long wavelength. For higher frequencies, the phase change increases while the distance of travel remains constant. Thus, the wavelength decreases, producing the wave compression effect seen in Fig. 6.

While the locust's TM shows some functional similarity to the basilar membrane of the mammalian cochlea, it clearly differs in many respects. The main functional difference is the way that the locust membrane compresses a large range of frequencies into a short spatial dimension. On the basilar membrane, a continuous gradient of stiffness contributes to the arising of travelling waves, spreading the amplitude maxima along its length and thus spreading the different frequency components along a series of distinct topographical locations.

For the locust, a more abrupt change in stiffness can be expected that presumably contributes to generating possibly only two types of travelling waves. Such dichotomy is reflected at another level of analysis, that of the locust's sensory ecology. The locust's auditory world seems to be split in two major categorical units comprising low and high frequency sounds. As in field crickets (Wyttenbach et al., 1996), the frequency parameter space in locusts seems to be divided in two logical categories, that of intra-specific communication and that of predator detection (Robert, 1989).

The locust's solution to the problem of mechanical and neural frequency analysis, as revealed by the present study, seems economical and elegant. A single morphological structure – the tympanal membrane – carries out both the functions of sound reception and frequency discrimination; converting acoustic energy into mechanical energy, and channelling the energy of specific frequencies to distinct neuron attachment locations.

Thanks go to J. Sueur and J. C. Jackson for their valuable comments on the manuscript. This work was funded by the Interdisciplinary Research Collaboration (IRC) in Nanotechnology (UK) and the Royal Society (London, UK).

References

Autrum, H. (1941) Ueber Gehör- und Erschütterungssinn bei Locustiden. *Z. Vergl. Physiol.* **28**, 580-637.

Breckow, J. and Sippel, M. (1985). Mechanics of the transduction of sound in the tympanal organ of adults and larvae of locusts. *J. Comp. Physiol. A* **157**, 619-629.

Cooper, N. P. and Rhode, W. S. (1992). Basilar membrane mechanics in the hook region of cat and guinea-pig cochleae: sharp tuning and nonlinearity in the absence of baseline position shifts. *Hear. Res.* **63**, 163-190.

Cooper, N. P. and Rhode, W. S. (1996). Fast travelling waves, slow travelling waves and their interactions in experimental studies of apical cochlear mechanics. *Auditory Neurosci.* **2**, 289-299.

Göpfert, M. C. and Robert, D. (2000). Nanometre-range acoustic sensitivity in male and female mosquitoes. *Proc. R. Soc. Lond. B. Biol. Sci.* **267**, 453-457.

Göpfert, M. C. and Robert, D. (2001). Active auditory mechanics in mosquitoes. *Proc. R. Soc. Lond. B. Biol. Sci.* **268**, 333-339.

Göpfert, M. C. and Robert, D. (2003). Motion generation by *Drosophila* mechanosensory neurons. *Proc. Natl. Acad. Sci. USA* **100**, 5514-5519.

Gray, E. G. (1960). The fine structure of the insect ear. *Philos. Trans. R. Soc. Lond. B. Biol. Sci.* **243**, 75-94.

Horridge, G. A. (1960). Pitch discrimination in Orthoptera (Insecta) demonstrated by responses of central auditory neurones. *Nature* **185**, 623-624.

Jacobs, K., Otte, B. and Lakes-Harlan, R. (1999). Tympanal receptor cells of *Schistocerca gregaria*: Correlation of soma positions and dendrite attachment sites, central projections and physiologies. *J. Exp. Zool. A* **283**, 270-285.

Kohllöffel, L. U. E. (1972). A study of basilar membrane vibrations. II. The vibratory amplitude and phase pattern along the basilar membrane (postmortem). *Acoustica* **27**, 66-81.

Kössl, M. and Boyan, G. S. (1998). Acoustic distortion products from the ear of a grasshopper. *J. Acoust. Soc. Am.* **104**, 326-335.

Michelsen, A. (1968). Frequency discrimination in the locust ear by means of four groups of receptor cells. *Nature* **220**, 585-586.

Michelsen, A. (1971). The physiology of the locust ear. I. Frequency sensitivity of single cells in the isolated ear, II. Frequency discrimination based upon resonances in the tympanum, and III. Acoustical properties of the intact ear. *Z. Vergl. Physiologie* **71**, 49-128.

Miller, L. A. (1977). Directional hearing in locust *Schistocerca gregaria* Forskal (Acrididae, Orthoptera). *J. Comp. Physiol.* **119**, 85-98.

Narayan, S. S. and Ruggero, M. A. (2000). Basilar-membrane mechanics at the hook region of the chinchilla cochlea. In *Recent Developments in Auditory Mechanics* (ed. H. Wada, T. Koike, T. Takasaka, K. Ikeda and K. Ohyama), pp. 95-101. Singapore: World Scientific.

Nobili, R., Mammano, F. and Ashmore, J. (1998). How well do we understand the cochlea? *Trends Neurosci.* **21**, 159-167.

Olson, E. S. (1999). Direct measurement of intra-cochlear pressure waves. *Nature* **402**, 526-529.

Olson, E. S. and Mountain, D. C. (1991). *In vivo* measurement of basilar-membrane stiffness. *J. Acoust. Soc. Am.* **89**, 1262-1275.

Ren, T. (2002). Longitudinal pattern of basilar membrane vibration in the sensitive cochlea. *Proc. Natl. Acad. Sci. USA* **99**, 17101-17106.

Rhode, W. S. (1971). Observations of the vibration of the basilar membrane in squirrel monkeys using the Mössbauer technique. *J. Acoust. Soc. Am.* **49**, 1218-1231.

Rhode, W. S. and Recio, A. (2000). Study of mechanical motions in the basal region of the chinchilla cochlea. *J. Acoust. Soc. Am.* **107**, 3317-3332.

Robert, D. (1989). The auditory behavior of flying locusts. *J. Exp. Biol.* **147**, 279-301.

Robert, D. and Lewin, A. (1998). Microscanning laser vibrometry applied to the biomechanical study of small auditory systems. *Proc. Int. Soc. Opt. Eng.* **3411**, 564-571.

Robles, L. and Ruggero, M. A. (2001). Mechanics of the mammalian cochlea. *Physiol. Rev.* **81**, 1305-1352.

Römer, H. (1976). Processing of information by tympanal receptors of *Locusta migratoria* (Acrididae, Orthoptera). *J. Comp. Physiol.* **109**, 101-122.

Russell, I. J. and Nilsen, K. E. (1997). The location of the cochlear amplifier: Spatial representation of a single tone on the guinea pig basilar membrane. *Proc. Natl. Acad. Sci. USA* **94**, 2660-2664.

Schwabe, J. (1906). Beiträge zur Morphologie und Histologie der tympanalen Sinnesapparate der Orthopteren. *Zoologica* **20**, 1-154.

Serbetcioglu, M. B. and Parker, D. J. (1999). Measures of cochlear travelling wave delay in humans: I. comparison of three techniques in subjects with normal hearing. *Acta Otolaryngol* **119**, 537-543.

Stephen, R. O. and Bennet-Clark, C. (1982). The anatomical and mechanical basis of stimulation and frequency analysis in the locust ear. *J. Exp. Biol.* **99**, 279-314.

von Békésy, G. (1960). *Experiments in Hearing*. New York: McGraw-Hill.

Wyttenbach R. A., May, M. L. and Hoy, R. R. (1996). Categorical perception of sound frequency by crickets. *Science* **273**, 1542-1544.